Integrated Analysis of Piping Systems

C.Y. Wang
Reactor Analysis and Safety Division, Argonne National Laboratory, 9700 South Cass Avenue, Argonne, Illinois 60439, U.S.A.

M.T. A-Moneim
Bell Laboratory, Naperville, Illinois 60540, U.S.A.

T.B. Belytschko
Department of Civil Engineering, The Technological Institute, Northwestern University, Evanston, Illinois 60201, U.S.A.

During accidental events the piping systems of nuclear reactors can be subjected to transient loadings of different types: (1) hydrodynamic loading resulting from pressure-wave propagation in the fluid, (2) thermal loading generated by fluid-temperature gradient, (3) structural loading during seismic events, and (4) pre-existent loads in the piping system due to normal operation pressurization, thermal and creep phenomena.

This paper describes a method for an integrated hydrodynamic-structural-thermal analysis of piping systems for the events mentioned above. The method couples 2-D implicit Eulerian finite-difference hydrodynamics with 3-D nonlinear, elastic-plastic finite element structural dynamics. The hydrodynamics utilizes the full Navier-Stokes equations, including the nonlinear convective and viscous terms. The structural analysis employs a 3-D pipe element with eight degrees of freedom per node (i.e., 3 displacements, 3 rotations, 1 membrane displacement, and 1 bending rotation) to account for the stresses arising from internal pressurization, as well as those arising from the flexural motion of the piping system.

The coupled fluid-structure model accounts for: (1) the correct interaction of the fluid mass with the structural mass, (2) the hydrodynamic forces on the structure resulting from elbows and tapers, (3) the motion of the Eulerian mesh with respect to the moving pipe, and (4) the effects of the pipe breathing mode on the hydrodynamics.

A thermal capability is also developed. It utilizes a 1-D energy equation for the fluid, in which the energy transfer between the fluid and the deforming pipe wall is accounted for. A 1-D radial heat conduction model is used to determine the temperature profile through the wall, which in turn will be used to estimate the thermal stresses.

The mathematical model used for the thermal stress calculation is applicable to the behavior of a large number of materials under a variety of loading conditions, such as thermal, plastic, and viscous effect. It is developed under the assumption of isotropy and a viscous condition that depends on the effective strain rate. The flow surface, which defines the purely elastic regime, can be arbitrarily small and an associated flow rule is employed for regimes of material plasticity.

Sample calculations illustrating the capabilities of the method and its resulting computer code are presented.

1. Introduction

The safety of piping systems during transients requires that there be no failure from the stresses arising from the pressure pulses introduced into the piping systems, as mentioned in the summary of this paper. To perform the structural analysis of piping systems, a piping program was initiated in the Reactor Analysis and Safety Division of Argonne National Laboratory. The ICEPEL code [1] was developed to perform a coupled hydrodynamic-structural analysis of piping systems in two dimensions. In this code, the Implicit Continuous-Fluid Eulerian finite difference hydrodynamics [2] is coupled to a nonlinear elastic-plastic explicit finite element model of the piping system using thin axisymmetric shell element and rigid co-rotational coordinate formulation [3].

Although the ICEPEL code can treat complex wave propagation in the piping system in two dimensions, it considers only the breathing mode of the pipes and components and ignores the bending of the pipes. Furthermore, the code requires the centerline of all pipes and components to be fixed in space and has no thermal-stress calculational capabilities.

In order to extend the ICEPEL to perform an integrity analysis of piping system, the structural capability has been improved considerably. A three-dimensional pipe element with eight degrees of freedom at each node was developed using a co-rotational coordinate formulation [4,5]. In addition, a spring element is used to model piping supports, such as snubbers and hangers.

In this paper, the coupling of the three-dimensional structural analysis to the two-dimensional hydrodynamics are addressed, together with the description of the capability for treating the thermal stress. Sample problems concerning validation of the fluid-structure-interaction and heat-conduction models are given.

The computer code, with the capability for treating fluid-structure-thermal interaction, is referred as SHAPS (Structural Hydrodynamic Analysis of Piping System).

2. Fluid-Structure Interaction

2.1 Inertia of the Fluid

Since the fluid is carried along with the moving pipe, the mass of the fluid should be combined with the mass of the structure, but only in some of the eight degrees of freedom. Figure 1 shows a generic pipe element in a general orientation with respect to the global-coordinate system (X, Y, and Z), where the mass of the fluid and the mass of the pipe are to be combined in the local $\hat{y}$ and $\hat{z}$ directions. Meanwhile, only the pipe mass is to be considered in the local $\hat{x}$ direction.

In the local-coordinate system, the contribution of an element to the translational mass at each of its nodes is represented by the diagonal mass matrix

$$[\hat{m}^t] = \begin{bmatrix} RT & 0 & 0 \\ 0 & RT + RTF & 0 \\ 0 & 0 & RT + RTF \end{bmatrix} , \qquad (1)$$

where RT is the mass of half the length of the element, and RTF is the mass of the fluid in half the length of the element.

In the global-coordinate system, the equivalent mass matrix is obtained using the transformation

$$[M^t] = [\mu][\hat{m}^t][\mu]^T \quad , \tag{2}$$

where $[\mu]$ is the direction cosine matrix of the local ($\hat{x}$, $\hat{y}$, and $\hat{z}$) system with respect to the global (X, Y, and Z) system. The mass matrix is used in the formulation of the equations of motion [5].

2.2 Hydrodynamic Force at Kinks

One hydrodynamic force contribution to the structure of a pipe system arises from elbows. An elbow is represented by a series of straight pipe segments; at each junction, the model includes "kinks" when force transfer occurs between the fluid and structure. At such kinks, two hydrodynamic forces result: a force due to the hydrodynamic pressure within the two elements connected through the node, and a force due to the change in the direction of the fluid element.

Figure 2 shows a typical case in which a kink in the piping system is developed between elements (k-1) and (k), which are connected through node N. Consider an infinitesimal region around N to represent a control volume that moves with node N in the global reference XYZ.

Because the infinitesimal mass of the control volume can be considered to be zero, the body, inertia, Coriolis, and centrifugal-force terms, as well as the rate of change of linear momentum inside the control volume, can be neglected. Hence, the momentum equation for the noninertial control volume can be shown to reduce to,

$$\sum \overline{F}_S = \text{momentum rate leaving control volume} - \text{momentum rate entering control volume.} \tag{3}$$

Equation (3) is to be applied in the three global coordinates X, Y, and Z.

The left-hand side of eq. (3) consists of two portions: the force from the pipe knee to the control volume (the reaction of the hydrodynamic force to the structure) and the force due to hydrodynamic pressures within elements (k-1) and k. Thus, in the global coordinate system, the left-hand side of eq. (3) is

$$F_S(i) = -F(i) + \left(e_1^{k-1}(i) - e_1^k(i)\right) A\, P_{J+1/2} \quad , \tag{4}$$

where i = 1, 2, and 3 for the global X, Y, and Z directions, $e_1^k(i)$ is the component of the unit vector e_1^k along the global i-direction, A is the pipe cross-sectional area, and $P_{J+1/2}$ is the hydrodynamic pressure at node N. F(i) is the global i-component of the hydrodynamic force on the node due to the kink, which has the form

$$F(i) = A\left[e_1^{k-1}(i) - e_1^k(i)\right]\left[P_{J+1/2} + \rho V_{J+1/2}\,|V_{J+1/2}|\right] \quad , \tag{5}$$

where i = 1, 2, and 3 for the global X, Y, and Z directions.

2.3 Effect of Pipe Motion on Hydrodynamics

As the pipe system moves in a three-dimensional space, it carries along with it the flowing fluid. The hydrodynamic finite-difference mesh is also assumed to be carried along with the pipe system without changing its shape or its size. Nevertheless, the fluid remains

free to slide along the pipe wall and the pipe remains free to twist independently of the fluid.

Let us consider a control volume V bounded by a surface S and moving with an arbitrary velocity $\overline{V}^G$. The conservation of mass and momentum of the fluid flowing through V are:

$$\frac{\partial \rho}{\partial t} + (\rho \overline{V}_i^D)_{,i} = 0 \quad \text{and} \quad \frac{\partial \rho \overline{V}_i}{\partial t} + (\rho \overline{V}_i \overline{V}_j^D)_{,j} + P_{,i} = 0 \quad , \tag{6}$$

where

$$\overline{V}^D = \overline{V} - \overline{V}^G \quad . \tag{7}$$

Equation (6) is written in the standard index notations. This equation indicate that only the convective terms are modified to accommodate the motion of the control volume V.

2.4 Pipe Breathing Mode

To account for the pipe-wall hoop motion in the hydrodynamics, we consider a free-slip fluid interface motion with respect to the pipe wall. Since the viscosity of the fluid (like water or sodium) is very small, the sliding boundary condition is used at the interface which requires that the fluid be allowed to slide along the interface, but in the normal direction, the fluid and the structure are forced to move together.

A relaxation equation is used to adjust iteratively the pressure in the fluid-structure-interface zone so that the sliding boundary condition is rigorously satisfied [1,6].

3. Thermal Analysis

3.1 Energy Equation

One capability has been introduced in the SHAPS code pertains to the treatment of the thermal shock that could be experienced by the primary piping system due to either cooling fluctuations in the core or the pre-existing thermal gradient during the normal operating condition. Here a one-dimensional energy equation is developed that provides temperature distribution in the piping system. The energy equation that accounts the energy transfer between the fluid and the deforming pipe wall is

$$\rho c \frac{\partial T}{\partial t} = k \frac{\partial^2 T}{\partial z^2} - \rho v c \frac{\partial T}{\partial z} - \left\{ p + 1/2\ \rho v^2 - (\lambda + 2\mu) \frac{\partial v}{\partial z} \right\} \frac{\partial v}{\partial z} + \frac{2}{R} \left[h_i (T_1^W - T) - P_B u^W \right] \quad , \tag{8}$$

where ρ is the density; c the specific heat constant; T the temperature; v the axial fluid velocity; p the pressure; λ and μ the viscosity coefficients; R the pipe inner radius; h_i the coefficient of heat transfer at the inside surface of the wall; T_1^W the wall temperature at the inner surface; P_B the pressure at the pipe boundary; u^W is the wall radial velocity.

3.2 Heat-Conduction Model

The heat conduction model of the SHAPS code utilizes a one-dimensional radial heat conduction equation to determine the temperature profile through the wall. This equation is

$$\rho c \frac{\partial T}{\partial t} = \frac{1}{r} \frac{\partial}{\partial r} \left(kr \frac{\partial T}{\partial r}\right) \quad . \tag{9}$$

Then for isotropic homogeneous materials, the thermal conductivity can be factored out of the right hand side term.

To obtain the temperature distribution throughout the pipe wall, eq. (9) is written into finite-difference form with respect to the control volume shown in Fig. 3. The resulting difference equation is solved implicitly by applying the convective boundary conditions at both inner and outer surfaces of the pipe.

3.3 Thermal-Stress Calculation

The mathematical model for the thermal-stress analysis is applicable to the behavior of a large number of materials under a variety of loading conditions, such as thermal, plastic, and viscous effects. This model is termed as "thermo-viscoplastic" even though elastic behavior is also included. The basis of the approach is to solve the flow condition

$$p = \bar{\sigma} - H\left(\bar{e}^{i}, \dot{\bar{e}}^{i}, T\right) = 0 \quad , \tag{10}$$

in which $\bar{\sigma}$ and H denote the effective stress and flow stress, respectively; $\bar{e}^{i}$ and $\dot{\bar{e}}^{i}$ are the effective inelastic strain and its rate; T is the temperature.

A modified Newton-Raphson procedure is applied directly to the yield criterion given in eq. (10) to evaluate stress and strain for given total and thermal strains. Material properties are described by numerical data and linear interpolation in a two-dimensional space provides the required functions. Detailed descriptions of this model are presented in Ref. [7].

4. Sample Problems

4.1 Experimental Validation of Fluid-Structure Interaction

Test FP-E-103 of a single elbow piping system is one of the simple elastic-plastic piping experiments performed by SRI International [8] for verifying the two-dimensional code ICEPEL. The same test is analyzed here using the new three-dimensional coupled code SHAPS. The purpose of this analysis is (1) to validated the fluid-structure interaction scheme, (2) to investigate the flexural response of a single elbow configuration to internally propagating pressure pulses, and (3) to estimate the pressure attenuation along the elbow. Since the entire results are quite voluminous only important portions are presented here.

A schematic of the experimental layout and the instrumentation locations of test FP-E-103 is shown in Fig. 4. A specially designed and calibrated pulse gun is directly flanged to a thick-walled stainless steel pipe of 8.26 cm (3.25 in) outside diameter, 0.48 cm (0.188 in) wall thickness, and 304.8 cm (10 ft) length. This pipe is directly flanged to a thin-walled Nickel-200 test pipe which is 152.4 cm (5 ft) long and has an outside diameter of 7.62 cm (3 in) and a wall thickness of 0.165 cm (0.065 in). The thin-walled test pipe is connected in series to identical pipe through a 90° thick-walled stainless steel elbow of 11.43 cm (4.5 in) radius of curvature and 0.762 cm (0.3 in) wall thickness. The second flexible pipe ended with a heavy blind flange.

In the vicinity of the elbow, the comparisons between the calculated and the measured pressure histories for gages P8-P10 upstream from the elbow and gages P14-P16 downstream from it are shown in Figs. 5 and 6. In addition to the good agreement, it should be noted that the calculated peak pressure downstream from the elbow is about 3.35 MPa, which is slightly

less than the calculated peak upstream from the elbow of about 3.61 MPa. The pressure drop is about 7%, compared to the measured drop of about 18%.

It should also be noted that the two-dimensional ICEPEL computations which ignore the motion of the elbow showed [9]: (a) no drop in the peak pressure along the elbow, and (b) slightly higher pressure levels -- of about 4 MPa -- in the pipes as well as in the elbow. Similar results were obtained from the three-dimensional SHAPS computations when the elbow nodes were constrained. Therefore, it is concluded that the calculated drop in peak pressure is due to the motion of the elbow in response to the propagating pressure waves.

4.2 Test of Heat-Conduction Model

The heat conduction model used in the SHAPS code has been tested against three simple problems where the steady state analytical solutions can be readily obtained by integrating the heat conduction equation. Three problems considered are (1) a rectangular slab, (2) a thin-wall pipe with thickness to radius ratio (t/R) equals to 0.0433, and (3) a thick-wall pipe with t/R ratio equals to 0.433. In all three problems, the inner surface is assumed to be kept at 100°F, while the outer surface is maintained at 0°F. The thickness of the wall in these three problems is assumed to be equal to 2 ft. Temperature profiles are calculated by the SHAPS code at eight equally spaced temperature nodes. All computations are carried out to 150 and 300 hrs, with a time step equal to 0.5 hour.

The steady state analytical solutions and SHAPS' transient solutions concerning the temperatures at 8 different nodes are given in Fig. 7. As can be seen that (1) the solutions of the thin wall pipe compare very well with the slab solutions. This means that if the pipe wall is very thin (t/R is small) the effect of curvature on the temperature distribution becomes insignificant. However, for the case of the thick-walled pipe where t/R is large, the temperature difference at the corresponding stations deviated significantly from those of the slab and thin-wall pipe solution. Also, as expected, at the later stage (say 300 hr) the results of the transient calculations compared remarkably well with the respective analytical solutions.

4. Conclusions

A new three-dimensional code, SHAPS, for the coupled hydrodynamic-structural-thermal analysis of piping systems has been developed. It has been applied to a simple elastic-plastic single elbow piping experiment. The calculations compared favorably with the experimental measurements. Moreover, the calculations showed that an attenuation in peak pressure along the elbow. This pressure attenuation results from the motion of the elbow. The heat conduction model also has been checked out against three simple problems with steady state analytical solutions. The calculated temperatures at late stages of the transient compared very well with analytic, steady-state solutions.

With the analytical development to be made in a continuous and progressive manner, the SHAPS code promises to be a significant step toward obtaining a better structural-hydrodynamic-thermal analysis of complex piping systems under dynamic loading condition. Piping system supports and external loading, as well as thermal transients, can be considered in addition to the loading from internally propagating pressure pulses.

Acknowledgments

This work is performed in the Engineering Mechanics Program of the Reactor Analysis and Safety Division of Argonne National Laboratory under the auspices of the U.S. Department of Energy.

References

[1] A-MONEIM, M. T., "Coupled Hydrodynamic-Structural Response Analysis of Piping Systems," ANL-77-91 (February, 1978).

[2] HARLOW, F. H., AMSDEN, A. A., "A Numerical Fluid Dynamics Calculation Method for All Flow Speeds," J. of Computational Physics 8, pp. 197-213 (1971).

[3] BELYTSCHKO, T. B., HSIEH, B. J., "Non-linear Transient Analysis of Shells and Solids of Revolution by Convected Coordinates," AIAA/ASME/SAE 14th Structure, Structural Dynamics and Material Conference, Williamsburg, VA, March 20-22, 1973.

[4] BELYTSCHKO, T. B., SHWER, L., KLEIN, M. J., "Large Displacement, Transient Analysis of Space Frames," Int. J. of Numerical Methods in Eng. 11, pp. 65-84 (1977).

[5] A-MONEIM, M. T., "Three Dimensional Finite Element Formulation for Elastic-Plastic Non-linear Analysis of Piping Systems," Nuclear Technology 51, No. 3, pp. 464-475 (1980).

[6] WANG, C. Y., "Analysis of Nonlinear Fluid-Structure Interaction Transient in Fast Reactors," ANL-78-103, ANL Report (November, 1979).

[7] SCHREYER, H. L., "Theory and Constitutive Equation Subroutine for Thermo-Viscoplasticity," ANL/RAS 80-15, Argonne National Laboratory (July, 1980).

[8] CAGLIOSTRO, D. J., ROMANDER, C. M., "Experiments on the Response of Flexible Piping Systems to Internal Pressure Pulses," SRI Fourth Interim Report on Project PVD-1960, SRI International, Menlo Park, CA (April 1976).

[9] A-MONEIM, M. T., "ICEPEL Analysis of and Comparison with Simple Elastic-Plastic Piping Experiments," ANL-78-105 (December, 1978).

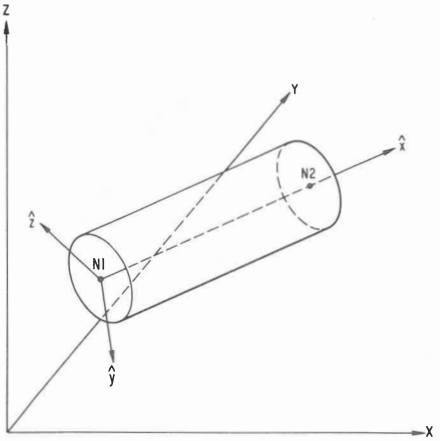

1. Local Coordinates for a Generic Pipe Element.

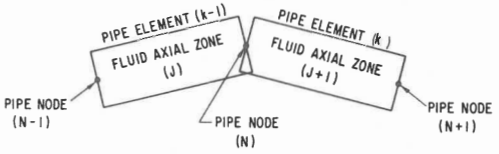

2. Typical Pipe Kink.

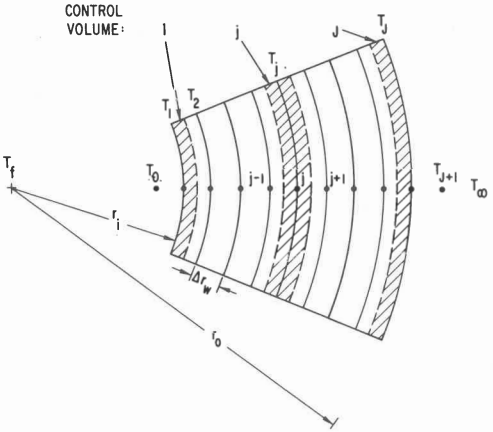

3. Control-Volume Used to Derive the Finite-Difference Heat Conduction Equation.

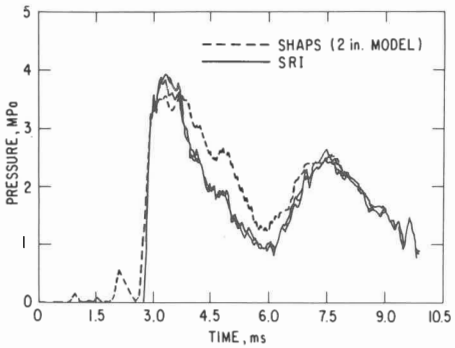

5. Comparison of the Calculated and Measured Pressure-Time Histories at Gauges P8-P10 of the First Pipe Before the Elbow.

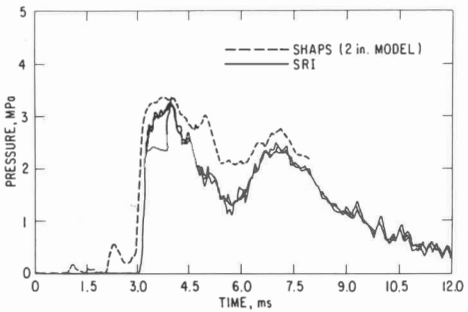

6. Comparison of the Calculated and Measured Pressure-Time Histories at Gauges P14-P16 of the Second Pipe After the Elbow.

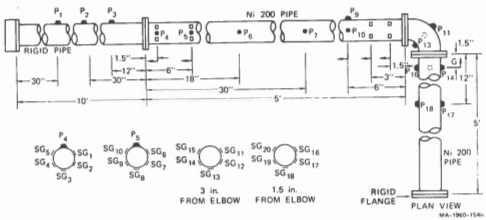

4. Layout of the SRI Pipe-Elbow Experiment FP-E-103.

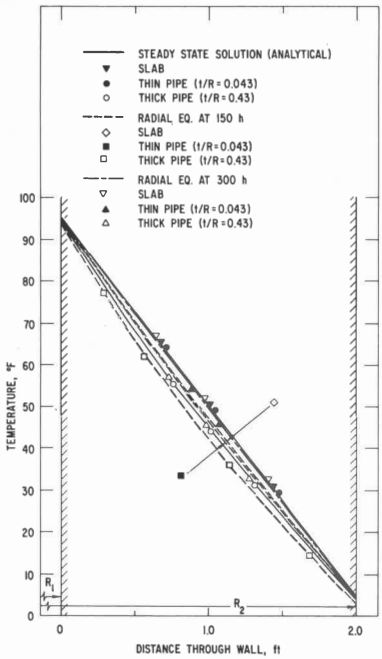

7. Temperature Profiles Due to Heat Conduction for Various Cases of the Three Problems Studied.